

Discontinuous switching of position of two coexisting phases

Samuel Krüger,^{1,2,3} Christoph A. Weber,^{1,3,4} Jens-Uwe Sommer,^{2,5,3} and Frank Jülicher^{1,3}

¹*Max Planck Institute for the Physics of Complex Systems,
Nöthnitzer Str. 38, 01187 Dresden, Germany*

²*Leibniz-Institut für Polymerforschung, Dresden 01069, Germany*

³*Center for Advancing Electronics Dresden cfAED, Dresden, Germany*

⁴*Division of Engineering and Applied Sciences,
Harvard University, Cambridge, MA 02138, USA*

⁵*TU Dresden, Institute for Theoretical Physics, Zellescher Weg 17, 01069 Dresden*

Abstract

Here we investigate how the positions of a condensed phase can be controlled by using concentration gradients of a regulator that influences phase separation. We consider a mean field model of a ternary mixture where a concentration gradient of a regulator is imposed by an external potential. We show that novel first order phase transition exists at which the position of the condensed phase switches in a discontinuous manner. This mechanism could have implications for the spatial organization of biological cells and provides a control mechanism for droplets in microfluidic systems.

PACS numbers: 47.55.D-, 64.75.Xc, 87.15.Zg

Phase separation of a mixture refers to the formation of a condensed phase that coexists with a dilute phase of lower concentration [1, 2]. Such demixing is the result of a first order thermodynamic phase transition where the concentration difference between the phases changes discontinuously. It can be observed in many forms in everyday life, for example when oil is added to water. The occurrence of a transition from the homogeneous mixture to a system with coexisting phases can be controlled by temperature or by changing the composition of the mixture. Condensed phases are influenced by surfaces possibly causing wetting transitions [3–5]. Furthermore, phase separation can be affected by external forces such as gravity causing sedimentation.

A key question is how condensed phases such as droplets are positioned in systems with external cues like concentration gradients or external fields. The study of positioning of phases provides general insights in the physics of phase separation of spatially inhomogeneous systems. Understanding the underlying mechanism of the positioning of condensed phases may open the possibility of applications in microfluidic devices. Positioned condensed phases could be used to seal and open junctions at specific locations in the microfluidic device, or simply position chemicals that enrich in the condensed or dilute phase. The positioning of condensed phases in a complex mixture also plays a role in cell biology. In particular, positioned condensed phases are used to segregate molecules during asymmetric cell division [6–9].

Here we study the equilibrium physics of the positioning of two condensed phases in inhomogeneous systems. We present a simplified model that provides the basic mechanism for the positioning at thermal equilibrium which can be further extended to non-equilibrium processes such as the kinetics of droplet formation and ripening. In our model phase separation of two components is subject to a concentration gradient of a *regulator component* where the gradient is generated by an external field. The regulator component affects demixing of the two components but does not phase separate itself. The system then relaxes to a spatially inhomogeneous thermodynamic equilibrium state with two coexisting phases positioned by the regulator gradient. The spatial distributions of the three concentration profiles at thermal equilibrium are determined by minimizing a mean field free energy functional. We find that as a function of an interaction parameter the position of the condensed phase switches discontinuously from a position in the region of large regulator concentration (correlated state) to the region of low regulator concentration (anti-correlated). This switching

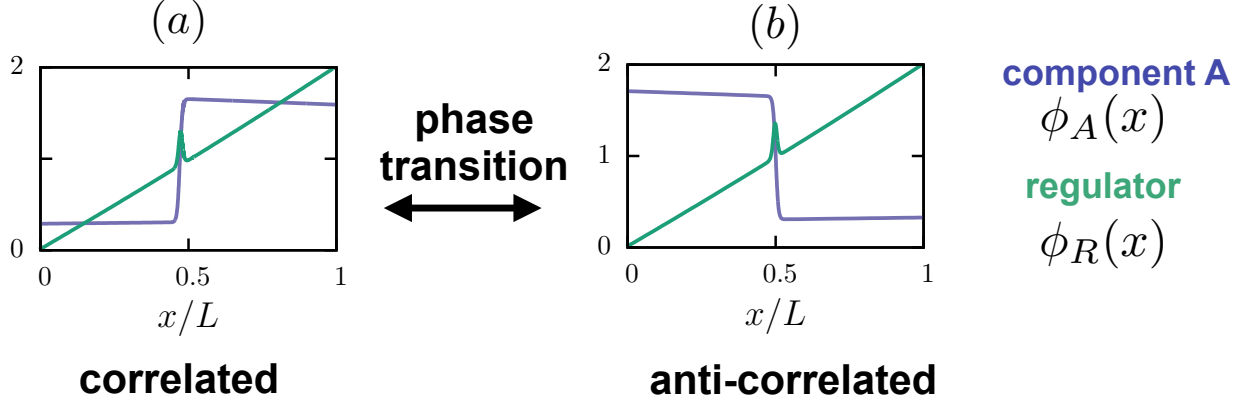


FIG. 1. Spatial regulation of phase separation by a discontinuous phase transition. (a,b) The regulator (green) forms a gradient due to an external potential. Depending on the interactions with the regulator the spatial distribution of e.g. component A (purple; component B behaves oppositely) switches from a spatially correlated (a) to an anti-correlated (b) distribution with respect to the regulator. The switch corresponds to a discontinuous phase transition.

of position corresponds to a novel, equilibrium first order phase transition at which an order parameter undergoes a jump (Fig. 1(a,b)).

In our equilibrium model for spatial regulation of phase separation we consider three components [10]: two components which can demix from each other, A and B , and a regulator R that interacts with these components. The regulator affects phase separation but does not demix from A and B . Demixing and interactions with the regulator are described by the Flory-Huggins free energy density for three components ([11, 12] and Supplemental Material [13], II):

$$\begin{aligned}
 f(\phi_A, \phi_R) = \frac{k_b T}{\nu} & \left[\sum_{i=A,B,R} \phi_i \ln \phi_i + \chi_{AR} \phi_A \phi_R \right. \\
 & + \chi_{BR} \phi_R \phi_B + \chi_{AB} \phi_A \phi_B + (U/k_b T) \phi_R \\
 & \left. + \frac{\kappa_R}{2} |\nabla \phi_R|^2 + \frac{\kappa_A}{2} |\nabla \phi_A|^2 + \frac{\kappa}{2} \nabla \phi_R \nabla \phi_A \right].
 \end{aligned} \tag{1}$$

We consider the incompressible system in which the molecular volumes are equal to ν and $\phi_B = 1 - \phi_R - \phi_A$. The logarithmic contributions correspond to the mixing entropy, while the second line in Eq. (1) describes the molecular interactions between the components; χ_{ij} is the interaction parameter between component i and j . The gradient terms represent

contributions to the free energy associated with spatial inhomogeneities. They introduce two length scales, $\sqrt{\kappa_A}$ and $\sqrt{\kappa_R}$. The regulator R is subject to an external field described by a position-dependent potential $U(x)$. For simplicity we consider in the following a one-dimensional system and choose a potential of the form $U(x) = -k_b T \ln(1 + s(2x - L))$, where $s > 0$ characterizes the slope of the potential and its inverse is a third length scale in our model. Note that in the absence of A and for $\phi_R \ll \phi_B$, $\phi_R(x)$ attains a concentration profile that is linear in space with a slope s . We consider a finite system of size L and two type of boundary conditions: (i) Neumann boundary conditions, $\phi'_i(0) = \phi'_i(L) = 0$, for all fields, where the primes denote spatial derivatives, and (ii) periodic boundaries with $\phi_i(0) = \phi_i(L)$ and $\phi'_i(0) = \phi'_i(L)$. The conditions (i) imply that there is no explicit energetic bias to wet or dewet the boundary, but the presence of the boundary enforces the slopes of the concentration profiles close to the boundary. In contrast, the periodic conditions (ii) allow to study the system in the absence of boundaries.

To calculate the equilibrium profiles $\phi_A(x)$ and $\phi_R(x)$, we minimize the free energy

$$F[\phi_A(x), \phi_R(x)] = \int_0^L dx f(\phi_A(x), \phi_R(x), x). \quad (2)$$

Due to particle number conservation, two constraints are imposed for the minimization: Each field ($i = A, R$) obeys $\bar{\phi}_i = L^{-1} \int_0^L dx \phi_i(x)$, where $\bar{\phi}_i$ are the average volume fractions and $\bar{\phi}_B = 1 - \bar{\phi}_A - \bar{\phi}_R$. Variation of the free energy Eq. (2) with the constraints of particle number conservation implies ($i = A, R$):

$$0 = \int_0^L dx \left(\frac{\partial f}{\partial \phi_i} - \frac{d}{dx} \frac{\partial f}{\partial \phi'_i} + \lambda_i \right) \delta \phi_i + \frac{\partial f}{\partial \phi'_i} \delta \phi_i \Big|_0^L, \quad (3)$$

where λ_R and λ_A are Lagrange multipliers, and the prime denotes a derivative with respect to x . The boundary terms vanish for both, Neumann and periodic boundary conditions. Using the explicit form of the free energy density (Eq. (1)), the Euler-Lagrange equations can be derived (see Supplemental Material [13], I). We solve these equations using a finite difference solver (bvp4c in MATLAB [14]). As control parameters we consider the three interaction parameters χ_{AR} , χ_{AB} and χ_{BR} , the slope of the external potential s and the mean volume fraction of A -material, $\bar{\phi}_A$. The mean regulator material is fixed to $\bar{\phi}_R = 0.02$ in all presented studies. Moreover, we focus on the limit of strong phase segregation where the interfacial width is small compared to the system size, i.e. $\sqrt{\kappa_i} \ll L$. In this limit, we verified that our results depend only weakly on the specific values of κ_i .

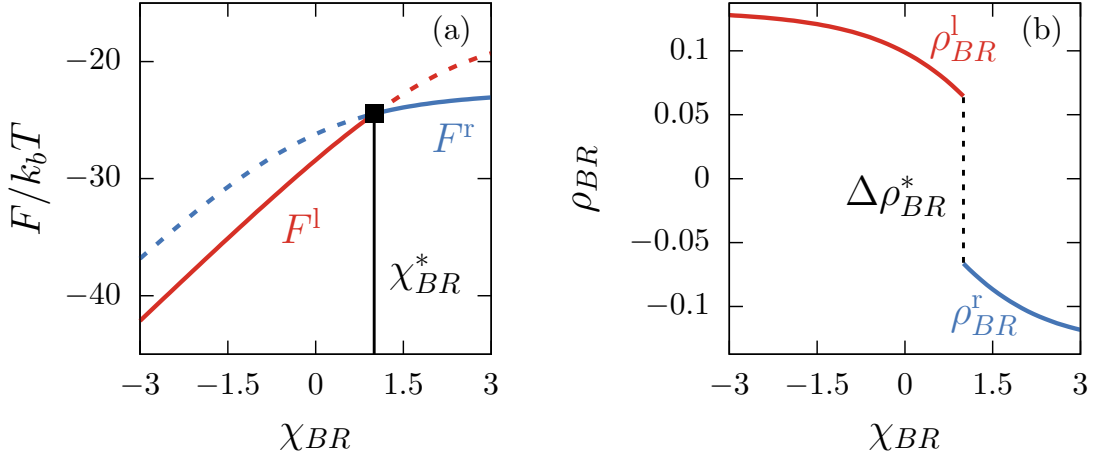


FIG. 2. Discontinuous phase transition. (a) Free energy F (Eq. (2)) as a function of the R - B interaction parameter χ_{BR} . F^l and F^r are the free energies of the correlated and anti-correlated stationary solution with respect to the regulator gradient, respectively (Fig. 1(a,b)). Lines are dashed when solutions are metastable. At χ_{BR}^* , F^l and F^r intersect causing a kink corresponding to the solution of lowest free energy. This shows that the transition between correlation and anti-correlation is a discontinuous phase transition. (b) The order parameter ρ_{BR} (Eq. (4)) jumps at χ_{BR}^* by a value of $\Delta\rho_{BR}^*$. The transition point χ_{BR}^* does not depend on the slope of the regulator s , while χ_{BR}^* increases linearly with s (see Supplemental Material [13], VI) Parameters: $\chi_{AB} = 4$, $\chi_{AR} = 1$, $\bar{\phi}_A = 0.5$, $\bar{\phi}_R = 0.02$, $\kappa_R/L^2 = 7.63 \cdot 10^{-5}$, $\kappa_A/L^2 = 6.10 \cdot 10^{-5}$, $\kappa/L^2 = 6.10 \cdot 10^{-5}$, $Ls = 0.99$. For plotting, $\nu = L/256$ was chosen.

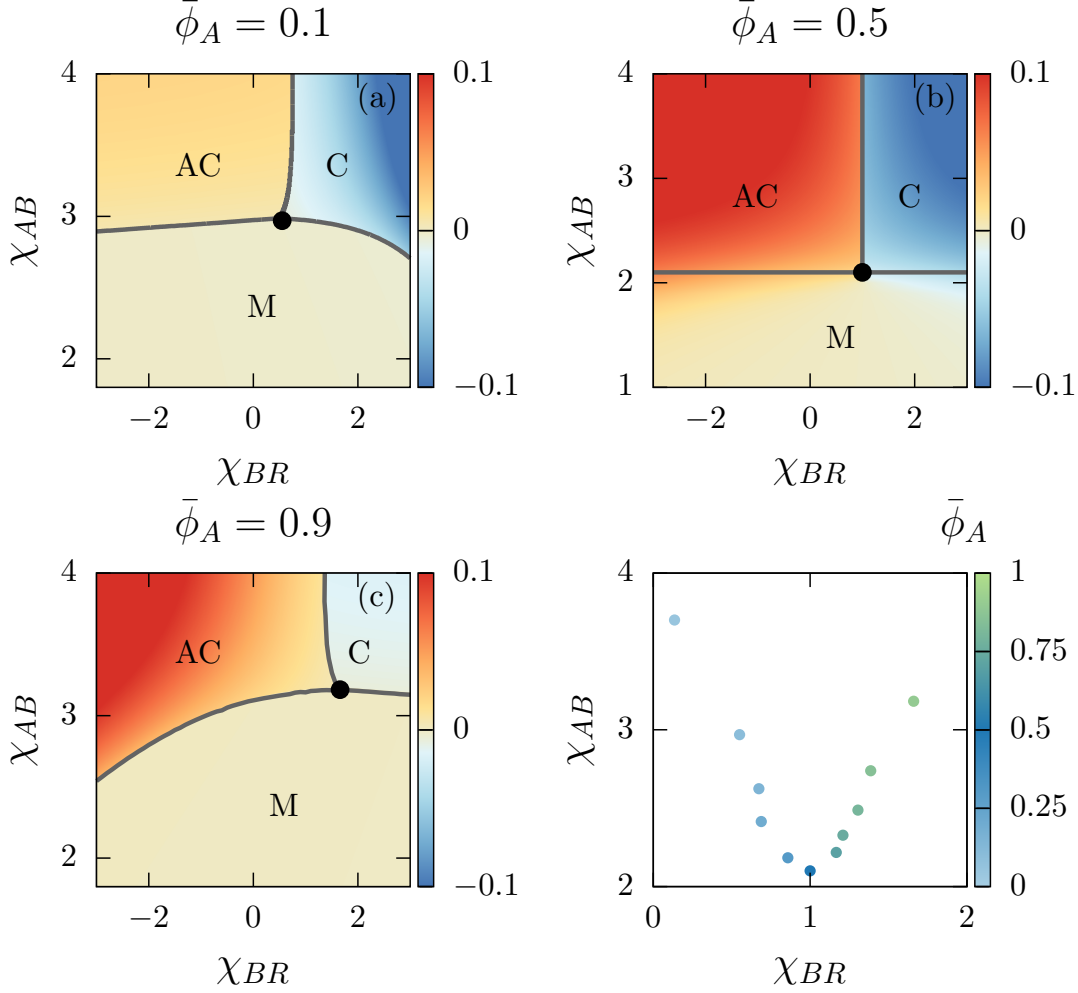


FIG. 3. Phase diagrams of our ternary model with spatial regulation. (a-c) Phase diagram for three volume fractions $\bar{\phi}_A = \{0.1, 0.5, 0.9\}$ and varying the interaction parameters χ_{AB} and χ_{BR} . The color code depicts the order parameter ρ_{BR} defined in Eq. (4). Component A is spatially correlated (C) with the regulator profile if $\rho_{BR} < 0$, and anti-correlated (AC) otherwise. When the system is mixed (M), $\rho_{BR} \approx 0$, and spatial profiles of all components are only weakly inhomogeneous (no phase separation). The solid black line in (a) is the transition line between C and AC calculated with the ansatz Eq. (6) using condition (5). The triple point (black dot) corresponds to the point in the phase diagrams where the three regions meet and the three free energies are equal. (d) Triple point for different $\bar{\phi}_A$ values (color code). Parameters: $\chi_{AR} = 1$, $\bar{\phi}_R = 0.02$, $\kappa_R/L^2 = 7.63 \cdot 10^{-5}$, $\kappa_A/L^2 = 6.10 \cdot 10^{-5}$, $\kappa/L^2 = 6.10 \cdot 10^{-5}$, $Ls = 0.99$, $\nu = L/256$.

Solving the Euler-Lagrange equations with Neumann boundary conditions (i), we find two spatially inhomogeneous solutions for component A , which we denote $\phi_A^l(x)$ and $\phi_A^r(x)$, and the two corresponding solutions for the regulator component R , are denoted $\phi_R^l(x)$ and $\phi_R^r(x)$ (the profile of B follows from volume conservation). The phase separating material A is either accumulated close to the right boundary of the system ($\phi_R^r(x)$ and $\phi_A^r(x)$) and correlated with the concentration of the regulator material (Fig. 1(a)), or it is accumulated at the left ($\phi_R^l(x)$ and $\phi_A^l(x)$) and anti-correlated with the regulator (Fig. 1(b)). Upon varying the interaction parameters χ_{BR} in Fig. 7(a,b), the free energies of the correlated and the anti-correlated states, $F^r = F[\phi_A^r, \phi_R^r]$ and $F^l = F[\phi_A^l, \phi_R^l]$, are different. They intersect at one point $\chi_{BR} = \chi_{BR}^*$ (Fig. 7(a)). At this point the lowest free energy exhibits a kink, which means that the system undergoes a discontinuous phase transition when switching from the spatially anti-correlated ('left') to the spatially correlated ('right') solution with respect to the regulator. A set of order parameters suitable to study this phase transition is

$$\begin{aligned} \rho_{ij} &= (k_b T L \mathcal{N}_{ij} / \nu)^{-1} \frac{d}{d\chi_{ij}} [F(\phi_i(x), \phi_j(x)) - F(\bar{\phi}_i, \bar{\phi}_j)] \\ &= \mathcal{N}_{ij}^{-1} \int_0^L dx (\phi_i(x)\phi_j(x) - \bar{\phi}_i\bar{\phi}_j), \end{aligned} \quad (4)$$

where the squared normalization $\mathcal{N}_{ij}^2 = \text{Var}(\phi_i^\Theta)\text{Var}(\phi_j^\Theta)$ with $\text{Var}(\phi_i) = \int_0^L dx (\phi_i^2(x) - \bar{\phi}_i^2)$, denoting the variance and $\phi_i^\Theta(x) = \Theta(L\bar{\phi}_i - x)$, where $\Theta(\cdot)$ denotes the Heaviside step function. This normalization ensures that $-1 < \rho_{ij} < 1$ and $\rho_{ij} = \pm 1$ if $\phi_i(x) = \phi_i^\Theta(x)$. The derivative of the free energy with respect to the interaction parameter χ_{ij} generates the covariance between the spatially dependent fields $\phi_i(x)$ and $\phi_j(x)$. If the fields are spatially correlated, $\rho_{ij} > 0$, and if they are anti-correlated, $\rho_{ij} < 0$. For homogeneous fields with $\phi_i(x) = \bar{\phi}_i$, $\rho_{ij} = 0$. Varying the interaction parameter χ_{BR} (Fig. 7(b)), the order parameters ρ_{BR} and ρ_{AR} jump at the threshold value χ_{BR}^* , while in the absence of a regulator gradient ($s = 0$), they change smoothly. The jump of both order parameters in the presence of a regulator gradient indicates that the spatial correlation of A and B to R changes abruptly, which is expected in case of a first order phase transition.

By means of the order parameter ρ_{BR} (Eq. (4)) we can now discuss the phase diagrams as a function of the interaction parameters for different volume fractions of the demixing material, $\bar{\phi}_A$. We find three regions (Fig. 3(a-c)): A mixed region (M), where volume fraction profiles are only weakly inhomogeneous and no phase separation occur. In addition, there

are two regions, (C) and (AC), where components A and B phase separate and A is spatially correlated or anti-correlated with the regulator R , respectively. There exists a triple point where all three states have the same free-energy. For $\bar{\phi}_A = 1/2$, the shape of the transition line between correlated and anti-correlated states is straight and χ_{BR}^* is independent of χ_{AB} (Fig. 3(b)). If $\bar{\phi}_A$ is decreased, the region of the correlated state in the phase diagram grows. In this case, the correlated state is favored, while for increasing $\bar{\phi}_A$, the anti-correlated state is preferred. The transition line to the mixed states is horizontal for $\bar{\phi}_A = 1/2$ (Fig. 3(b)). For both, larger and smaller $\bar{\phi}_A$ -values, it becomes curved and moves towards larger χ_{AB} interaction parameters. This behavior can be qualitatively understood by the upshift of the demixing threshold χ_{AB} once $\bar{\phi}_A$ deviates from $1/2$, as known for binary systems. Since the concentration of R is small here, this analogy provides a good approximation ($\bar{\phi}_R \rightarrow 0$ in Eq. (1)). Both trends explain the parabolic shape of the positions of the triple point in the phase diagrams when $\bar{\phi}_A$ is varied (Fig. 3(d)).

The transition line in the phase diagrams between the correlated and anti-correlated solution as a function of the interaction parameters can be estimated analytically. In the absence of a regulator gradient ($s = 0$), the free energies of both solutions are the same for all interaction parameters for which phase separation occurs. In the presence of a regulator gradient, however, the free energies corresponding to the correlated and the anti-correlated solutions are unequal for most points in the phase diagram. The reason is that the external potential $U(x)$ forces the regulator to form a gradient, and thus the interactions with the regulator lead to different free energies of the correlated and anti-correlated states. Only along the transition line between both states the free energies equal:

$$\Delta F = F[\phi_A^r, \phi_R^r] - F[\phi_A^l, \phi_R^l] = 0. \quad (5)$$

This condition can be used to estimate the transition line for varying interaction parameters and the slope of the potential, s . To estimate ΔF we parametrize the profiles of the stationary solutions $\phi_A^{r,l}(x)$ and $\phi_R^{r,l}(x)$ using physical assumptions that are in agreement with our numerical results. First we idealize the already narrow interface of the demixed component ϕ_A as sharp. Since the regulator is maintained by the external potential, we find $\phi_R^r(x) \simeq \phi_R^l(x)$ close to the transition line. Thus we use the one profile, denoted as $\phi_R(x)$, for both regulator states. In addition, we approximate the regulator profile as linear function with slope m , neglecting spatial non-linearities that can be seen in Fig. 1(a,b). The

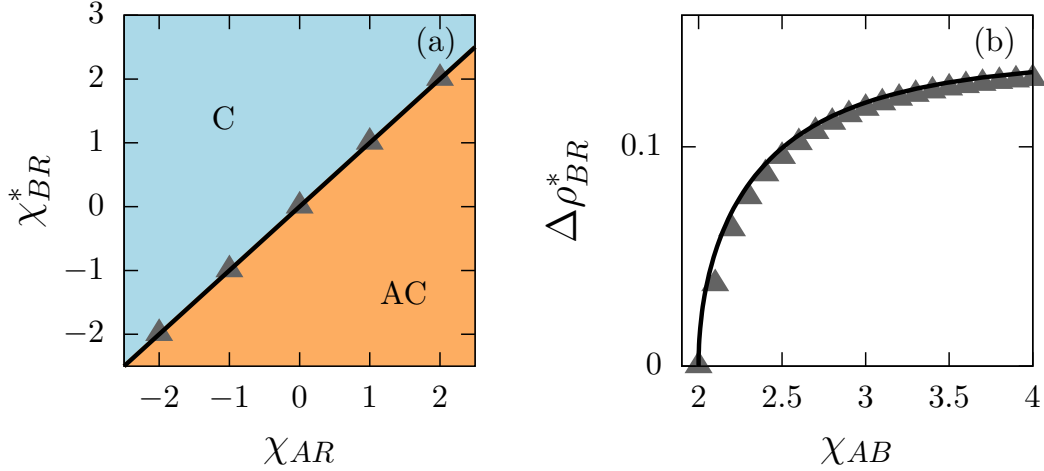


FIG. 4. Phase diagrams and order parameters estimated by ansatz Eq. (6). (a) The transition between spatial correlation (C) and anti-correlation (AC) of the distribution of component A with respect to the regulator in the χ_{AR} - χ_{BR} -plane. Parameters: $\chi_{AB} = 4$, $\bar{\phi}_A = 0.5$, $\bar{\phi}_R = 0.02$, $\kappa_R/L^2 = 7.63 \cdot 10^{-5}$, $\kappa_A/L^2 = 6.10 \cdot 10^{-5}$, $\kappa/L^2 = 6.10 \cdot 10^{-5}$, $Ls = 0.99$, $\nu = L/256$. (b) Jump of the order parameter at the transition point, $\Delta \rho_{BR}^*$, as a function of the interaction parameter χ_{AB} . Additionally to the parameters of (a), $\chi_{AR} = 1$ and $\chi_{BR} = 1$. The black line in (a) and (b) shows the result obtained from using Eq. (6); the triangles are numerical results from the minimization of Eq. (2).

low volume fractions outside the condensed phase of the demixed binary A - B system are approximated as constant values $\tilde{\phi}_{\text{out}}$. The larger volume fraction (inside) shows a weakly linear profile (Fig. 1(a,b)). For most parameters, the volume fraction inside the condensed phase can be well described as $\phi_{\text{in}}(x) = \tilde{\phi}_{\text{in}} - \phi_R(x)$, where $\tilde{\phi}_{\text{in}}$ is the constant volume fraction inside the condensed phase of the binary A - B mixture (see Supplemental Material [13], V). The approximated profiles are:

$$\phi_A^l(x) = \left[\phi_{\text{in}}(x) - \tilde{\phi}_{\text{out}} \right] \Theta(\epsilon_l - x) + \tilde{\phi}_{\text{out}}, \quad (6a)$$

$$\phi_A^r(x) = \left[\phi_{\text{in}}(x) - \tilde{\phi}_{\text{out}} \right] \Theta(\epsilon_r - L + x) + \tilde{\phi}_{\text{out}}, \quad (6b)$$

$$\phi_R(x) = m(x - L/2) + \bar{\phi}_R. \quad (6c)$$

The conservation of A determines the domain sizes $\epsilon_{l,r}$ of the phase separated region (see Supplemental Material [13], IV). To calculate ΔF (Eq. (5)), the free energy density (Eq. (1))

is integrated in the domain $[0, L]$. Using the approximated profiles (Eqs. (6)) we find

$$\Delta F \simeq \frac{k_b T}{\nu} \frac{\chi_{BR} - \chi_{AR}}{12} m \mathcal{G}, \quad (7)$$

where the value \mathcal{G} depends only on the parameters of the simplified solutions (see Supplemental Material [13], IV). Consistently, $\Delta F = 0$, if there is no regulator gradient ($m = 0$). In presence of a regulator gradient, $\Delta F = 0$ if $\chi_{BR}^* = \chi_{AR}$, which defines the transition line between the correlated and anti-correlated solution obtained from the parametrized solutions Eqs. (6). This prediction is in very good agreement with our numerical results for $\bar{\phi}_A \simeq 1/2$; see black lines in Fig. 3(a) and Fig. 4(a). By means of the ansatz given in Eqs. (6) we can also estimate how the jump of the order parameter $\Delta\rho_{BR}^*$ (definition see Fig. 7(b)) at the transition point depends on the model parameters. In particular we find that the estimated $\Delta\rho_{BR}^*$ as a function of the slope of the regulator (not shown) and the interaction parameter χ_{AB} (Fig. 4(b)) almost perfectly describe the data obtained from the numerical minimization of the free energy. This shows that the proposed parametrization of the stationary solutions represents a consistent approximation. We conclude that the positioned and phase separated profiles possess a sharp interface and the volume fraction inside has a weak linear slope that is mainly determined by volume exclusion with the regulator.

The phase diagrams (Fig. 3) depend on the boundary conditions rising the question whether the boundary play a key role for the existence of the phase transition. To this end we considered a periodic system without boundaries. We find that the reported first order transition also exists for in the absence of boundaries (see Supplemental Material [13], III). Thus the transition is not induced by boundaries as for example in the case of wetting transitions [3–5].

The discontinuous switching of phase separation could be tested experimentally. A soluble salt of high magnetic susceptibility could be used to create and maintain concentration gradients via the application of an inhomogeneous magnetic field [15]. Phase separation in a regulator gradient could be observed by introducing components that phase separate in a salt dependent manner. In particular, a pre-formed droplet could be added to an existing regulator gradient or the regulator gradient is created after Ostwald-ripening is completed [16–19]. The phase transition could be triggered by changing the concentrations of the phase separating material, by changing the temperature or by adding additional components that influence the interaction parameters. The systems considered here could

also be relevant for applications. As the composition of a condensed phase creates a distinct chemical environment, our work may provide a novel mechanism to control and switch chemical environments in microfluidic devices.

We would like to thank Martin Elstner and Omar Adame for fruitful and stimulating discussions. This project was supported by the Center for Advancing Electronics Dresden (cfAED). Christoph A. Weber thanks the German Research Foundation (DFG) for financial support. Samuel Krüger and Christoph A. Weber contributed equally to this work.

SUPPLEMENTAL MATERIAL

Euler-Lagrange Equations

From the variation of the free energy and the explicit form of the free energy density (main text, Eq.(1)), we find the following set of the Euler-Lagrange equations:

$$\begin{aligned}
0 = & \left(\kappa_A \kappa_R - \frac{\kappa^2}{4} \right) \phi_A'' - \kappa_R \left(\lambda_A + \chi_{AB} (1 - 2\phi_A) + \chi \phi_R \right. \\
& + \ln \left(\frac{\phi_A}{1 - \phi_A - \phi_R} \right) \Big) + \frac{\kappa}{2} \left(\lambda_R + U_R + \chi_{BR} (1 - 2\phi_R) \right. \\
& \left. + \chi \phi_A + \ln \left(\frac{\phi_R}{1 - \phi_A - \phi_R} \right) \right), \tag{8a}
\end{aligned}$$

$$\begin{aligned}
0 = & \left(\kappa_A \kappa_R - \frac{\kappa^2}{4} \right) \phi_R'' - \kappa_A \left(\lambda_R + U_R + \chi_{BR} (1 - 2\phi_R) \right. \\
& + \chi \phi_A + \ln \left(\frac{\phi_R}{1 - \phi_A - \phi_R} \right) \Big) + \frac{\kappa}{2} \left(\lambda_A + \chi_{AB} (1 - 2\phi_A) \right. \\
& \left. + \chi \phi_R + \ln \left(\frac{\phi_A}{1 - \phi_A - \phi_R} \right) \right). \tag{8b}
\end{aligned}$$

Here, we defined $\chi = \chi_{AR} - \chi_{AB} - \chi_{BR}$ and rescaled length $x \rightarrow x L$.

Penalty of spatial inhomogeneities in the ternary Flory-Huggins free energy density

Derivation using a mean field approximation

To show this relation, we start from the local mean-field free energy on the lattice and calculate the continuum limit of this free energy as shown in Ref. [20] for a binary system. The local free energy density of the three component system is derived in [21, 22] using a mean-field approximation:

$$\begin{aligned}
\frac{f\nu}{k_B T} = & \sum_{\alpha} (\phi_A(\alpha) \ln \phi_A(\alpha) + \phi_R(\alpha) \ln \phi_R(\alpha) + (1 - \phi_A(\alpha) - \phi_R(\alpha)) \ln (1 - \phi_A(\alpha) - \phi_R(\alpha))) \\
& + \frac{1}{2} \sum_{\alpha, \beta \text{ with } \alpha \neq \beta} (J_{AB}(\alpha, \beta) \phi_A(\alpha) (1 - \phi_A(\beta) - \phi_R(\beta)) \\
& + J_{BR}(\alpha, \beta) \phi_R(\alpha) (1 - \phi_A(\beta) - \phi_R(\beta)) + J_{AR}(\alpha, \beta) \phi_A(\alpha) \phi_R(\beta)) , \tag{9}
\end{aligned}$$

where ν is the molecular volume. The greek indices α and β indicate the positions on the lattice. The first line describes the entropy of the mixture. Each contribution is local. The

second and third line contains the energetic part of the free energy. It describes the non-local interactions between neighboring lattice sites.

In the next steps we will perform the continuum limit. In case of the entropic contribution, we can simply replace $\phi_i(\alpha) \rightarrow \phi_i(x)$. In case of the energetic contributions, we rearrange the terms leading to:

$$\begin{aligned} \frac{1}{2} \sum_{\alpha, \beta \text{ with } \alpha \neq \beta} [J_{AB}(\alpha, \beta) \phi_A(\alpha) (1 - \phi_A(\beta)) + J_{BR}(\alpha, \beta) \phi_R(\alpha) (1 - \phi_R(\beta)) \\ + (J_{AR}(\alpha, \beta) - J_{AB}(\alpha, \beta) - J_{BR}(\alpha, \beta)) \phi_A(\alpha) \phi_R(\beta)] . \end{aligned} \quad (10)$$

Each contribution can be rewritten as

$$J_{AB}(\alpha, \beta) \phi_A(\alpha) (1 - \phi_A(\beta)) \quad (11)$$

$$= \frac{1}{2} J_{AB}(\alpha, \beta) [(\phi_A(\alpha) - \phi_A(\beta))^2 - (\phi_A(\alpha))^2 - (\phi_A(\beta))^2 + 2\phi_A(\alpha)] ,$$

$$J_{BR}(\alpha, \beta) \phi_R(\alpha) (1 - \phi_R(\beta)) \quad (12)$$

$$= \frac{1}{2} J_{BR}(\alpha, \beta) [(\phi_R(\alpha) - \phi_R(\beta))^2 - (\phi_R(\alpha))^2 - (\phi_R(\beta))^2 + 2\phi_R(\alpha)] ,$$

$$\begin{aligned} [J_{AR}(\alpha, \beta) - J_{AB}(\alpha, \beta) - J_{BR}(\alpha, \beta)] \phi_A(\alpha) \phi_R(\beta) \\ = \frac{1}{2} [J_{AR}(\alpha, \beta) - J_{AB}(\alpha, \beta) - J_{BR}(\alpha, \beta)] [\phi_A(\alpha) \phi_R(\alpha) + \phi_A(\beta) \phi_R(\beta) \\ - (\phi_A(\alpha) - \phi_A(\beta)) (\phi_R(\alpha) - \phi_R(\beta))] . \end{aligned} \quad (13)$$

We can identify the Flory Huggins interaction parameter as $\chi_{ij} = \frac{1}{2} \sum_{\beta} J_{ij}(\alpha, \beta)$. In the continuum limit we can introduce the gradient of the volume fractions as $(\phi_i(\alpha) - \phi_i(\beta)) \rightarrow a \nabla \phi_i$. We finally obtain the free energy $F = \int dx f$ with the free energy density given as

$$f = f_0(x) + \frac{k_B T}{\nu} \left[\frac{\kappa_A}{2} |\nabla \phi_A(x)|^2 + \frac{\kappa_R}{2} |\nabla \phi_R(x)|^2 + \frac{\kappa}{2} \nabla \phi_A(x) \nabla \phi_R(x) \right] , \quad (14)$$

where

$$\begin{aligned} \frac{f_0 \nu}{k_B T} = \phi_A(x) \ln \phi_A(x) + \phi_R(x) \ln \phi_R(x) + (1 - \phi_A(x) - \phi_R(x)) \ln (1 - \phi_A(x) - \phi_R(x)) \\ + \chi_{AR} \phi_A(x) \phi_R(x) + \chi_{AB} \phi_A(x) (1 - \phi_A(x) - \phi_R(x)) + \chi_{BR} \phi_R(x) (1 - \phi_A(x) - \phi_R(x)) . \end{aligned} \quad (15)$$

The parameters characterizing the penalty corresponding to spatial inhomogeneities are $\kappa_i = a^2 \chi_{iB}$, $i \in \{A, R\}$, and $\kappa = a^2 (\chi_{AR} - \chi_{AB} - \chi_{BR})$.

Phenomenological derivation

In the Ginzburg-Landau free energy the penalties corresponding to spatial inhomogeneities are phenomenologically introduced based on symmetry considerations:

$$f - f_0 = \frac{\tilde{\kappa}_A}{2} (\nabla \phi_A)^2 + \frac{\tilde{\kappa}_B}{2} (\nabla \phi_B)^2 + \frac{\tilde{\kappa}_R}{2} (\nabla \phi_R)^2, \quad (16)$$

where $\tilde{\kappa}_i > 0$ since spatial inhomogeneities are unfavored. Moreover, f_0 is the free energy density that only depends on the volume fractions ϕ_i , $i \in A, B, R$. However, only two volume fraction fields are independent due to particle conservation and incompressibility, $1 = \phi_A + \phi_B + \phi_R$. Thus we can write $\nabla \phi_B = -\nabla \phi_A - \nabla \phi_R$, leading to

$$f - f_0 = \frac{\kappa_A}{2} (\nabla \phi_A)^2 + \frac{\kappa_R}{2} (\nabla \phi_R)^2 + \frac{\kappa}{2} \nabla \phi_A \nabla \phi_R. \quad (17)$$

Here, $\kappa_A = \tilde{\kappa}_A + \tilde{\kappa}_B$, $\kappa_R = \tilde{\kappa}_R + \tilde{\kappa}_B$ and $\kappa = \tilde{\kappa}_B$.

Choice of the parameters κ_i

In the presented studies, we have chosen $\kappa_A = \kappa$ for simplicity. Please note that the derivation presented in Sect. is based on a mean field approximation and therefore it should only serve as an estimate for the values κ_i . We chose the values for the parameters κ_A and κ_R consistent with these estimates (see figure captions in the main text).

Discontinuous phase transition in a periodic domain

Here we discuss the results of the minimization of the free-energy (Eq. (3), main text) using periodic boundaries with $\phi_i(0) = \phi_i(L)$ and $\phi'_i(0) = \phi'_i(L)$. We find the same main results as for Neumann boundary conditions, namely the existence of a discontinuous phase transition. In the periodic domain, we also use a periodic external potential:

$$U = -k_b T \ln \left(1 - A \sin \left(2\pi \left(\frac{x}{L} - \omega \right) \right) \right). \quad (18)$$

The parameter ω is a phase shift. The value of the phase is chosen such that the region of segregated A-material is placed at $x = 0$. The logarithmic form of the potential is chosen ensures that a sinus distribution of the regulator is obtained in the dilute limit. We find two stationary solutions of different spatial correlations with respect to the regulator. They

switch at χ_{BR}^* by a discontinuous phase transition (Fig. 5(a-c)). Therefore, a boundary of the system is not a necessary requirement for the emergence of the discontinuous phase transition discussed in our manuscript.

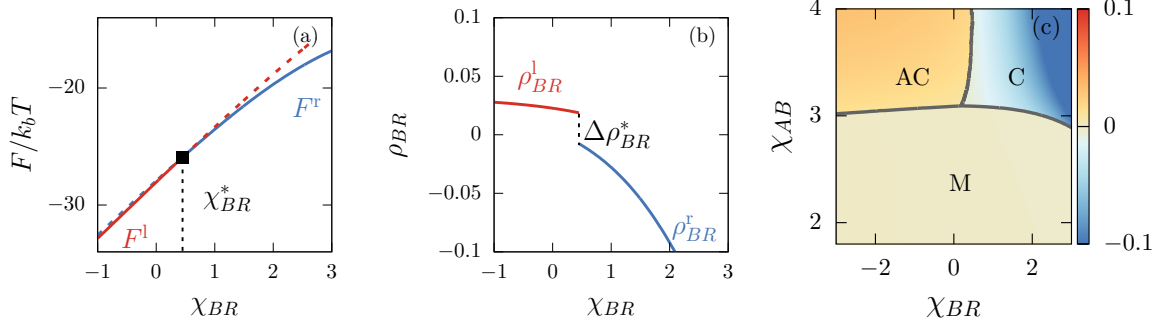


FIG. 5. Discontinuous phase transition in a periodic potential and periodic boundary conditions. (a) Free energy F as a function of the B - R interaction parameter χ_{BR} . F^l and F^r are the free energies of the correlated and anti-correlated stationary solution with respect to the regulator gradient, respectively. Lines are dashed when solutions are metastable. At χ_{BR}^* , F^l and F^r intersect and the solution of lowest free energy exhibits a kink. This shows that the transition between correlation and anti-correlation is a discontinuous phase transition. (b) The order parameter ρ^{RB} jumps at χ_{BR}^* by a value of $\Delta\rho_{BR}^*$. Parameters: $\chi_{AB} = 4$, $\chi_{AR} = 1$, $\bar{\phi}_A = 0.1$, $\bar{\phi}_R = 0.02$, $\kappa_R/L^2 = 7.63 \cdot 10^{-5}$, $\kappa_A/L^2 = 6.10 \cdot 10^{-5}$, $\kappa/L^2 = 6.10 \cdot 10^{-5}$, $A = 0.5$. For plotting, $\nu = L/256$ was chosen. (c) Phase diagrams of our ternary model for spatial regulation in a periodic potential and periodic boundary conditions ($\bar{\phi}_A = 0.1$). The color code depicts the order parameter ρ_{BR} . Component A is spatially correlated (C) with the regulator profile if $\rho_{BR} < 0$, and anti-correlated (AC) otherwise. When the system is mixed (M), $\rho_{BR} \approx 0$, and spatial profiles of all components are only weakly inhomogeneous (no phase separation). The triple point (black dot) corresponds to the point in the phase diagrams where the three regions meet and the three free energies are equal. Parameters: $\chi_{AR} = 1$, $\bar{\phi}_A = 0.1$, $\bar{\phi}_R = 0.02$, $\kappa_R/L^2 = 7.63 \cdot 10^{-5}$, $A = 0.5$, $\nu = L/256$.

Estimate of ΔF

The free energy difference between the two stationary solutions, ΔF , results from integration over the domain $[0, L]$ using the simplified solutions (Eqs. (7), main text):

$$\Delta F = \frac{k_b T}{\nu} \frac{\chi_{BR} - \chi_{AR}}{12} m \mathcal{G}, \quad (19)$$

where

$$\mathcal{G} = \left[12\epsilon_l (L - \epsilon_l) \left(2\tilde{\phi}_{\text{out}} + 2\bar{\phi}_R - 1 \right) + 3(L - 2\epsilon_l) \left(m(L - 2\epsilon_l) + 4\tilde{\phi}_{\text{out}} + 2\bar{\phi}_R - 2 \right) \Delta\epsilon \right] \quad (20)$$

and

$$\epsilon_l = \frac{-2 - Lm + 4\tilde{\phi}_{\text{out}} + 2\bar{\phi}_R}{2m} + \frac{\sqrt{8Lm \left(\tilde{\phi}_{\text{out}} - \bar{\phi}_A \right) + \left(2 + Lm - 4\tilde{\phi}_{\text{out}} - 2\bar{\phi}_R \right)^2}}{2m}, \quad (21)$$

$$\epsilon_r = \frac{-2 + Lm + 4\tilde{\phi}_{\text{out}} + 2\bar{\phi}_R}{2m} + \frac{\sqrt{8Lm \left(\bar{\phi}_A - \tilde{\phi}_{\text{out}} \right) + \left(-2 + Lm + 4\tilde{\phi}_{\text{out}} + 2\bar{\phi}_R \right)^2}}{2m}. \quad (22)$$

Here we substituted the interaction parameter between B and A by χ_{AB}^* , and truncated at $O(\Delta\epsilon)$ with $\Delta\epsilon = \epsilon_r - \epsilon_l$. Consistently, $\Delta F = 0$, if there is no regulator gradient ($m = 0$), and when phase separation is absent ($\epsilon_l = \epsilon_r = 0, L$). \mathcal{G} depends only of the parameters of the simplified solutions (see Eqs. (7), main text).

Comparison of simplified and full numerical solution

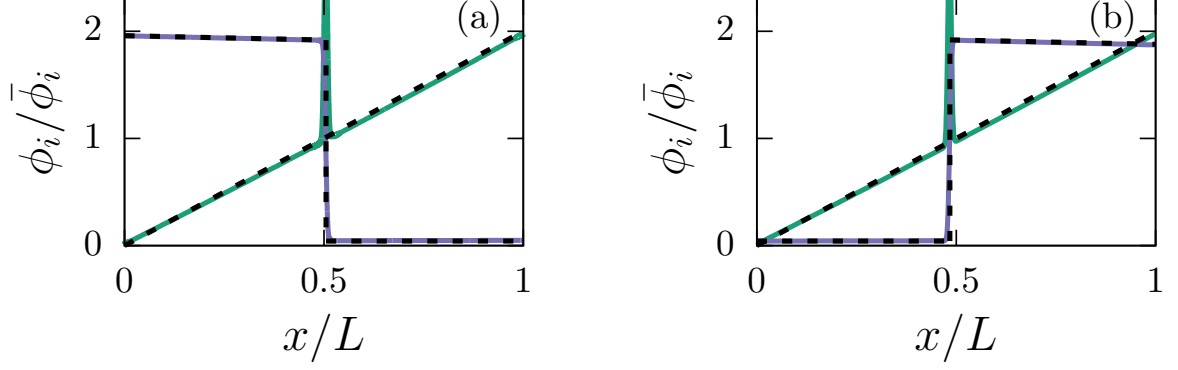


FIG. 6. (a) Anti-correlated profile and (b) Correlated profile close to the correlated-anti-correlated transition line. The dashed black lines depict the simplified profiles (Eqs. (7), main text) used in the analytic calculation of the free energy difference between the free energies of the two stationary solutions, ΔF . The peak of the regulator at the interface between the condensed and dilute phase is neglected in the analytical ansatz. Fixed parameters: $\chi_{AB} = 4$, $\chi_{AR} = 1$, $\chi_{BR} = 1$, $\bar{\phi}_R = 0.02$, $\phi_A = 0.5$, $\kappa_R/L^2 = 7.63 \cdot 10^{-5}$, $\kappa_A/L^2 = 6.10 \cdot 10^{-5}$, $Ls = 0.99$, $\nu = L/256$.

Transition point is independent of the regulator gradient

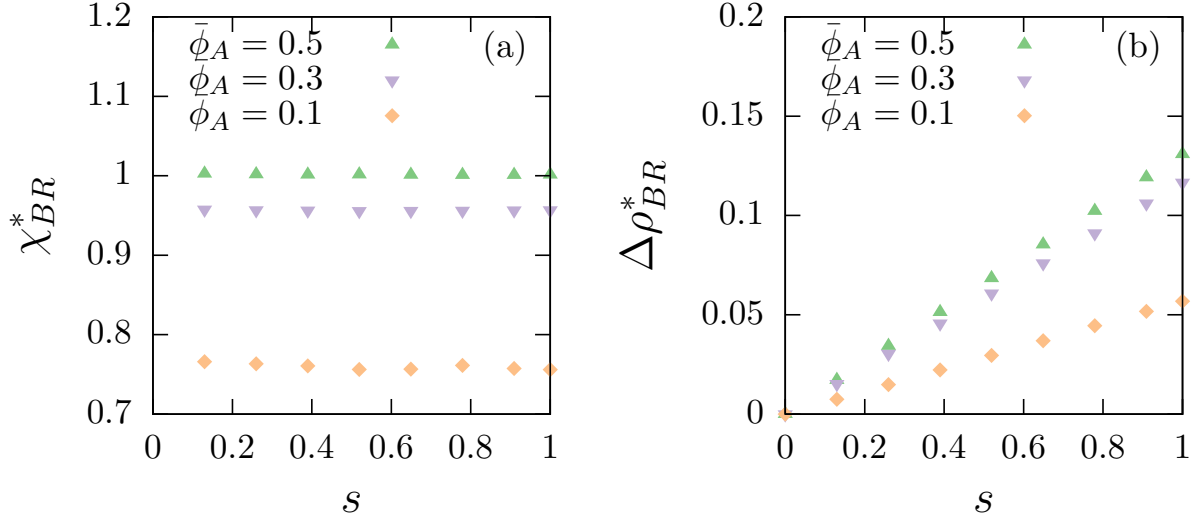


FIG. 7. (a) The transition point is independent on the slope of the regulator gradient s . (b) The jump of the order parameter at the transition point linearly increases with the slope of the gradient s . The slope of this linear dependence is influenced by $\bar{\phi}_A$. Fixed parameters: $\chi_{AB} = 4$, $\chi_{AR} = 1$, $\bar{\phi}_R = 0.02$, $\kappa_R/L^2 = 7.63 \cdot 10^{-5}$, $\kappa_A/L^2 = 6.10 \cdot 10^{-5}$, $\kappa/L^2 = 6.10 \cdot 10^{-5}$, $\nu = L/256$.

Regulator Peak at the Interface

The numerically obtained regulator profiles show a significant peak at the interface between the A-rich and the B-rich phase (see main text, Fig. 1(a,b)). The emergence of the regulator peak can be understood by entropic and energetic considerations of the free energy. For large and positive χ_{AR} and χ_{BR} (corresponding to a repulsive tendency with respect to the regulator), the energy of the system decreases as regulator accumulates at the interface. Moreover, the entropy decreases as the composition of the interfacial region of all three components is closer to a well-mixed state.

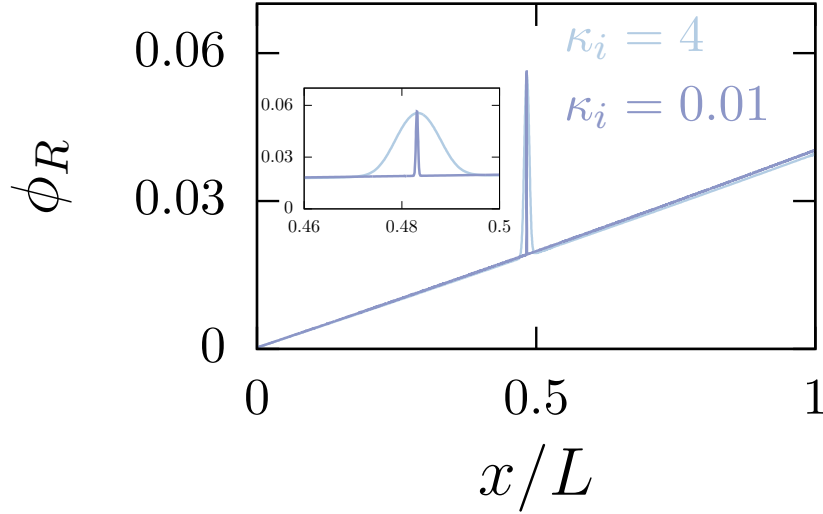


FIG. 8. Comparison of two regulator profiles of different κ_i parameters. The example $\kappa_i = 4$ is very close to set of parameters we generally use, where $\kappa_A = 4$, $\kappa = 4$ and $\kappa_R = 5$. The case $\kappa_i = 0.01$ is used as an example of small κ_i parameters. The plot shows that the peak area decreases if smaller κ_i are used. The smaller peak area is caused by a reduced peak width while the peak height is constant in good approximation. Fixed parameters: $\chi_{AB} = 4$, $\chi_{AR} = 1$, $\bar{\phi}_R = 0.02$, $\bar{\phi}_A = 0.5$, $s = 0.99$, $\nu = L/256$.

The amount of regulator material that is accumulated at the interface is strongly influenced by the κ_i -parameters; see Fig. 8. In Fig. 9 left, the peak area is shown for varying κ_i -parameters. For simplicity, we chose $\kappa_A = \kappa_R = \kappa$. The peak area vanishes as the κ_i -parameters approach zero. This behavior is expected since these parameters set the size of the interface between the phase separated phases. In this limit, the estimates for the phase boundaries based on the approximate solution (main text, Eq. (6)) are valid.

However, the peak height and thereby the existence of the peak is approximately independent of κ_i (Fig. 9 right). This indicates that the existence of the peak may depend on the interaction parameters for example. Since we also observed that the peak is more pronounced at the transition line between anti-correlated state and correlated state, we investigated the energetic influence on the peak height along the transition line. As derived in the main text, the transition line is governed by the condition $\chi_{AR} = \chi_{BR}$ for $\bar{\phi}_A = 0.5$. We find that the peak height increases as a function of the energetic parameters $\chi_{AR} = \chi_{BR}$ (Fig. 10). Large and positive values of χ_{AR} and χ_{BR} correspond to a repulsive tendency with respect to the regulator. This indicates that the energetic contribution to the free energy decreases as regulator accumulates at the interface.

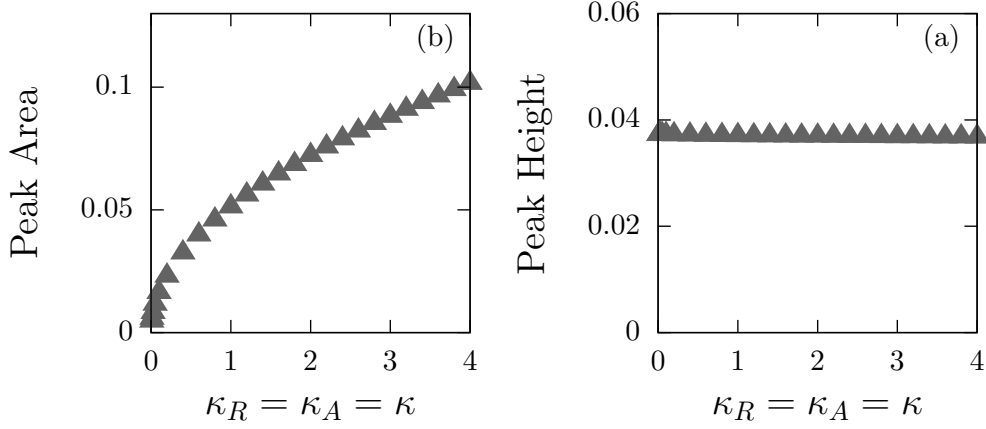


FIG. 9. Peak area (left) and peak height (right) as a function of the κ_i parameters. These two properties are measured without the linear regulator background. The peak height is a measure for the equilibrium value of the volume fraction of the regulator at the interface. The peak area measures the amount of regulator material accumulated at the interface. Here, the parameters κ_A , κ_R and κ are equal and changed simultaneously. The κ parameters have very minor influence on the peak height, it decreases only very slightly with increasing κ_i parameters. The influence of the κ_i parameters on the peak area is significant. The peak area decreases for smaller κ_i parameters. For very small κ parameters, the peak area is close to zero. Fixed parameters: $\chi_{AB} = 4$, $\chi_{AR} = 1$, $\bar{\phi}_R = 0.02$, $\bar{\phi}_A = 0.5$, $s = 0.99$, $\nu = L/256$.

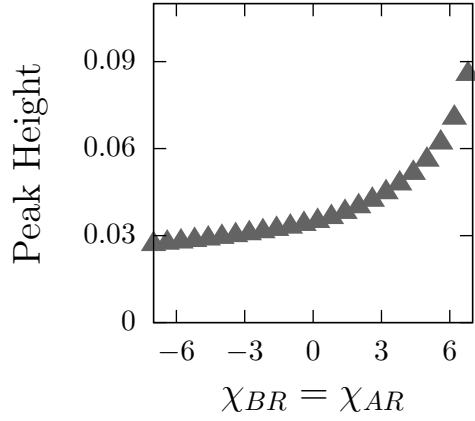


FIG. 10. Peak height for different Flory-Huggins parameters $\chi_{AR} = \chi_{BR}$. The peak height shows a monotonic growth for increasing $\chi_{AR} = \chi_{BR}$. The volume fraction of the regulator at the interface growth, if the energetic interaction of the regulator with the other components becomes more repulsive. Fixed parameters: $A = 0.0077$, $\chi_{AB} = 4$, $\bar{\phi}_R = 0.02$, $\bar{\phi}_A = 0.5$, $\kappa_R/L^2 = 7.63 \cdot 10^{-5}$, $\kappa_A/L^2 = 6.10 \cdot 10^{-5}$, $\kappa/L^2 = 6.10 \cdot 10^{-5}$, $\nu = L/256$.

-
- [1] A. Bray, *Advances in Physics* **43**, 357 (1994).
 - [2] A. Onuki, *Phase transition dynamics* (Cambridge University Press, 2002).
 - [3] J. W. Cahn, *The Journal of Chemical Physics* **66**, 3667 (1977).
 - [4] M. Moldover and J. W. Cahn, *Science* **207**, 1073 (1980).
 - [5] D. Pohl and W. Goldburg, *Physical Review Letters* **48**, 1111 (1982).
 - [6] C. P. Brangwynne, *Soft Matter* **7**, 3052 (2011).
 - [7] A. A. Hyman, C. A. Weber, and F. Jülicher, *Annual review of cell and developmental biology* **30**, 39 (2014).
 - [8] C. P. Brangwynne, P. Tompa, and R. V. Pappu, *Nature Physics* **11**, 899 (2015).
 - [9] S. Saha, C. A. Weber, M. Nusch, O. Adame-Arana, C. Hoege, M. Y. Hein, E. Osborne-Nishimura, J. Mahamid, M. Jahnel, L. Jawerth, *et al.*, *Cell* **166**, 1572 (2016).
 - [10] C. F. Lee, C. P. Brangwynne, J. Gharakhani, A. A. Hyman, and F. Jülicher, *Phys. Rev. Lett.* **111**, 088101 (2013).
 - [11] P. J. Flory, *The Journal of chemical physics* **10**, 51 (1942).
 - [12] M. L. Huggins, *The Journal of Physical Chemistry* **46**, 151 (1942), <http://dx.doi.org/10.1021/j150415a018>.
 - [13] See Supplemental Material for videos and more information at <http://...>
 - [14] J. Kierzenka and L. F. Shampine, *ACM TOMS* **27**, 299 (2001).
 - [15] M. Takayasu, R. Gerber, and F. Friedlaender, *IEEE Transactions on Magnetics* **19**, 2112 (1983).
 - [16] I. Lifshitz and V. Slyozov, *Journal of Physics and Chemistry of Solids* **19**, 35 (1961).
 - [17] C. Wagner, *Berichte der Bunsengesellschaft für physikalische Chemie* **65**, 581 (1961).
 - [18] J. H. Yao, K. Elder, H. Guo, and M. Grant, *Physical review B* **47**, 14110 (1993).
 - [19] C. A. Weber, C. F. Lee, and F. Jülicher, *New Journal of Physics* **19**, 053021 (2017).
 - [20] S. A. Safran, *Statistical Thermodynamics of Surface, Interfaces and Membranes* (Addison-Wesley Publishing Company, 1994).
 - [21] J. Sivardiere and J. Lajzerowicz, *Physical Review A* **11**, 2090 (1975).
 - [22] J. Sivardiere and J. Lajzerowicz, *Physical Review A* **11**, 2101 (1975).